PROCEEDINGS OF SPIE

Laboratory demonstration of a primary active mirror for space with the LATT: large aperture telescope technology

Briguglio, Runa, Biasi, Roberto, Gallieni, Daniele, Vettore, Christian, d'Amato, Francesco, et al.

SPIE.

Laboratory demonstration of a primary active mirror for space with the LATT: large aperture telescope technology

Runa Briguglio[a], Roberto Biasi[b], Daniele Gallieni[c], Christian Vettore[e], Francesco d'Amato[d], Marco Xompero[a], Carmelo Arcidiacono[a], Franco Lisi[a], Armando Riccardi[a], Christian Patauner[b], Paolo Lazzarini[c], Matteo Tintori[c], Fabrizio Duò[e], Mauro Pucci[d], Alessandro Zuccaro Marchi[f], and Luca Maresi[f]

[a]INAF Osservatorio Astrofisico Arcetri L. Enrico Fermi 5, 50125 Firenze, Italy
[b]Microgate, Via Stradivari 4, 39100 Bolzano, Italy
[c]ADS-International, via Roma 87, 23868 Valmadrera (LC), Italy
[d]CNR-INO, L.go E. Fermi 6, 50125 Firenze, Italy
[e]OHB CGS, Compagnia Generale per lo Spazio, Italy
[f]ESA/ESTEC, Keplerlaan 1, NL-2200 AG, Noordwijk, The Netherlands

ABSTRACT

The LATT project is an ESA contract under TRP programme to demonstrate the scalability of the technology from ground-based adaptive mirrors to space active primary mirrors. A prototype spherical mirror based on a 40 cm diameter 1 mm thin glass shell with 19 contactless, voice-coil actuators and co-located position sensors have been manufactured and integrated into a final unit with an areal density lower than 20 kg/m2. Laboratory tests demonstrated the controllability with very low power budget and the survival of the fragile glass shell exposed to launch accelerations, thanks to an electrostatic locking mechanism; such achievements pushes the technology readiness level toward 5. With this prototype, the LATT project explored the feasibility of using an active and lightweight primary for space telescopes. The concept is attractive for large segmented telescopes, with surface active control to shape and co-phase them once in flight. In this paper we will describe the findings of the technological advances and the results of the environmental and optical tests.

Keywords: Active Optics, Wavefront correctors, Deformable mirrors, Space telescopes, low-weight primary mirrors.

1. INTRODUCTION

The LATT project was born as a response to an ESA TRP call for the development of active mirrors for space telescopes. The project is a step forward after the ALC (Advanced Lidar Concept) study, where the possibility of using a deformable collecting element for LIDAR applications was addressed. More informations concerning the initial study may be found in.[1] The ancestor of LATT is however the adaptive secondary mirror developed for the adaptive optics facility at the Large Binocular Telescope in Arizona,[2] where a 1m size deformable secondary is controlled by voice coil actuators to close the adaptive optics (AO) loop with a pyramid wavefront sensor (WFS).

The LATT project gathered together italian industrial companies and research institutions in a consortium with the following tasks: initial study (from the ALC results); system design and components verification; prototyping of a demonstrator called LATT Optical BreadBoard (OBB); functional, verification and validation test on the demonstrator.

Since the beginning of the project, a few questions were considered the ultimate test-bench for the LATT approach to space active optics:

Further author information:
Runa Briguglio: E-mail: runa@arcetri.astro.it, Telephone: +39 055 2752200

- will a thin glass shell survive to the launch accelerations?

- is it possible to actively control the mirror with a very limited power budget?

- what is the final optical quality of a large format, ultra thin mirror controlled with few actuators?

- how lightweight can we go with such large format active mirror with a tight WF requirement?

The OBB is a 40 cm active mirror prototype integrated as the test facility to address these points and make a final assessment of the solutions proposed. The system was subjected to a test campaign including electro-mechanical and functional tests, thermo-vacuum, optical calibration and vibration test. After the integration and verification phase, we can claim that the points listed above have been positively answered and that the LATT approach to space active optics is robustly assessed. The project was concluded in October 2015 with the final review at ESA.

In the following we will overview the LATT way to space active optics (Sec.2) and describe the OBB (Sec.3) and the test campaign (Sec3.2). In the end we will summarize the most relevant results and discuss the outcomes and perspectives of the project. We will also discuss some possible system optimizations beyond the needs of the pure technical verification. In facts, the OBB is a concept demonstrator and, as such, many technical aspects have been addressed within the scope of the laboratory test, rather than as a flight unit.
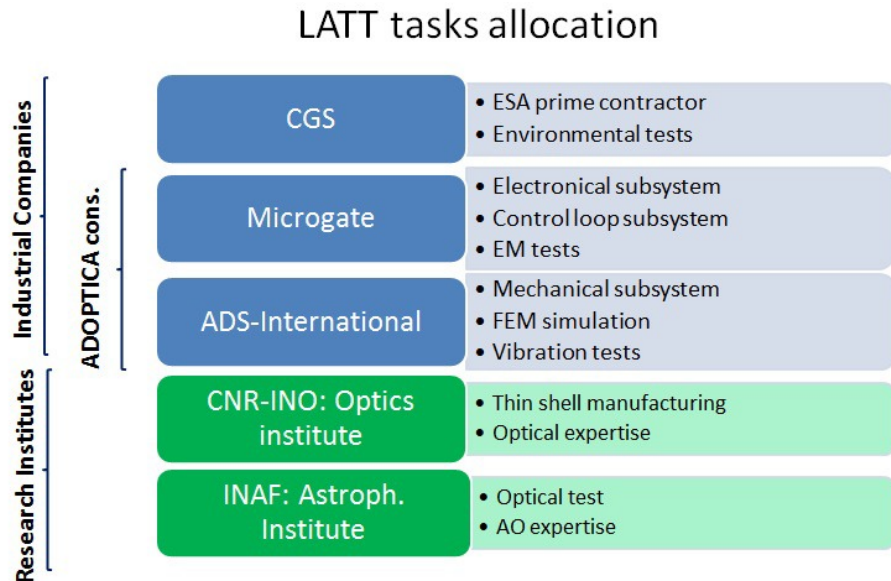

Figure 1. The partner of the LATT consortium with their work package within the project.

2. THE LATT CONCEPT

The background of the LATT is the development and operational expertise of the adaptive secondary mirror. With the LATT, the concept of the adaptive secondary was optimized to fit a space telescope as a deformable primary mirror.

The core of the system is a thin glass shell (TS), 1 to 2 mm thick, polished to match the prescription of the telescope optical design. The shell is actively shaped by voice coil actuators, housed on a reference body (RB) which provides also mechanical support to the system. The bending force is applied by means of magnetic interaction between the coil and a magnet glued on the back surface of the shell. Such contactless actuation mechanism makes voice coil actuators very attractive for space applications: in case of failure, the voice coil motor may simply be *de-activated*, without producing any local static warp on the optical surface. Suitable strategies for actuator *disabling* or *slaving* have been implemented and successfully tested for the Large Binocular Telescope

(LBT) and Very Large Telescope (VLT) secondary mirror.

Each LATT actuator is surrounded by a metal-coated armature that represents one electrode of a capacitor whereas the second electro is the backside of the TS that is as well metal coated. By inducing a reference signal on the shell coating and the capacitive coupling to the actuator armatures, a precise distance measurement is realized to provide a displacement reading. The actuator forces are therefore controlled in local close loop, fed by the capacitive sensors. Through the magnetic forces and the close loop, the TS floats at a *working distance* between 200 μm and 1200 μm from the RB. Such large gap allows the application of large amplitude commands and of global piston steps. The large stroke allowed for piston commands makes the LATT very suitable for segmented apertures; in this case the final deployment of the mirror segments and the fine phasing may be fully allocated to the actuators. The phasing of segments via voice coil actuators in optical close loop has been demonstrated in many laboratory tests. Such task has been also investigated for the ELT projects, where the low order modes application by segmented correctors requires precise pure piston and tilt commands, which is conceptually equivalent to phasing.

A second function of the metal coating of the backside of the TS is the electrostatic locking mechanism. Together with the front side of the RB that is as well metal coated and protected by an insulating layer, they form two electrodes of a capacitor. By applying a high voltage to these electrodes, an electrostatic force is pulling the TS towards the reference body. Therefore, the TS is fixed to the RB in order to withstand the large launch accelerations.

So far we mentioned the TS as the only optical element, while the RB is always detached from it. As a consequence, the requirements on the RB are dramatically reduced, opening the way to extremely lightweight materials for the bulk mechanical assembly, while the optical element is light by design: in the LATT, the glass itself accounts for less than 3 kg/m2 of the overall areal density. The LATT way offers simultaneous lightweight and active shape corrections, which are intimately related concepts. The OBB has an areal density lower than 17 kg/m2 and could be further optimized to reach 12 kg/m2.

Throughout the years, a well-established set of procedures and techniques has been developed for the adaptive mirrors. The LATT takes advantage of such expertise, for instance Finite Element Modeling, WF control and phasing algorithm, actuator management strategies, to address a number of system-wise aspects. They have been taken into account to give a global concept assessment, as reported in Sec.4.

3. THE LATT OBB

In order to demonstrate the LATT concept, a demonstration prototype (the OBB) was manufactured. It was not intended to be a flight unit, rather a test bed for answering the questions arose in Sec.1. In the following we will present a description of the mirror prototype and a resume of the test campaign.
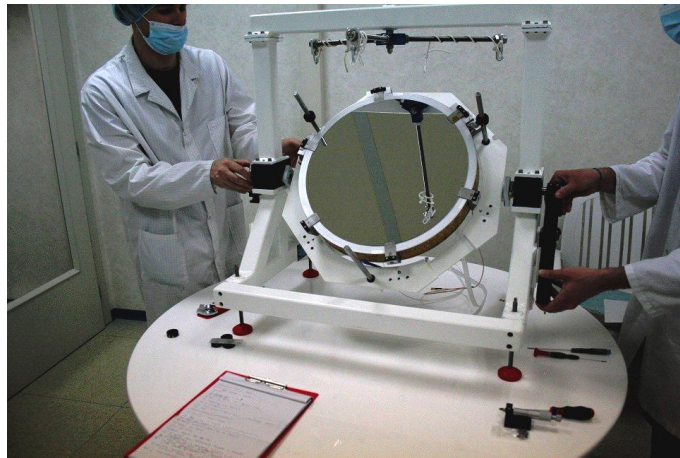

Figure 2. The OBB assembly on its integration stand, before the electromechanical tests.

Item	Value
General	
Mass areal density (as active M1)	16 kg/m2
ESLocking pressure	axial > 550 N/m2
	shear > 550 N/m2
Mirror assembly	
TS Material	Zerodur
TS Diameter	400.05±0.05 mm
TS Thickness	1.013 ± 0.001 mm
TS RoC	5000 mm ± 18mm
RB Material	Al Honeycomb + CFRP
RB coating	Protected Al + SiO_2
Actuators	
Stroke	$\pm500\mu m$
Precision	8nm RMS (typ)
Force budget	± 0.24 N
Open loop bandwidth	1.8 kHz
Power consumption	50-58 mW (per act.)
Mass	80g (per act.)

Table 1. Overview of the OBB characteristics.

Item	Shell 1	Shell 2
Diameter [mm]	400.0±0.05	400.0±0.05
Curv radius [mm]	5000±18	5000±18
Aver. Thickness [mm]	1.012	1.014
Thickness unif. [μm]	36 PtV	6 PtV
Micro-roughn. [nm]	1.5 RMS	1.8 RMS
WFE RMS (15Z)[nm]	38	72

Table 2. Manufacturing and polishing results of the two glass shells.

3.1 Components, manufacturing and assembling

3.1.1 The Thin Shell

The optical component to be actuated is a Zerodur^{TM} shell. The project specifications were: 40 cm diameter, 5000 mm curvature radius, 1 mm thickness. Two shells have been realized, starting from bulk disks, 42 cm diameter, 1.5 cm thickness. They have been first rough-cut and polished to obtain the concave surface, and reduced to the desired diameter. Then they have been rough-cut on the convex side, down to about 1.5 mm thickness, and finally polished to the desired thickness and surface quality. This procedure required attachment/detachment of the shell to/from suitable holders, using proper glues. Care has been taken to avoid sharp edges among the lateral surface and the two curved surfaces, where breaks could start. The final detachment of the thin, polished meniscus was made without any specific tool or machine, due to the limited dimensions of the two specimens. Both during machining, and for the final assessment of the shell specifications, the thickness was measured by using an optical gauge (Precitec CHRocodile S). Scratches and digs were verified by using a Nikon SMZ800 stereomicroscope, equipped with a Nikon Coolpix 4500 digital camera. The surface quality was assessed with a Zygo NewView 5000 3D surface profiler (Fig.3). The results of the test are visible in Table 3.1.1. We have checked each step of this procedure, in order to verify the scalability towards larger diameters. Just by building larger machines (which doesn't require any special technological breakthrough) we estimate that mirrors with one meter diameter are possible, while maintaining their thickness to one millimeter.

3.1.2 The Reference body

The backplane provides three different functions of the LATT system, namely:
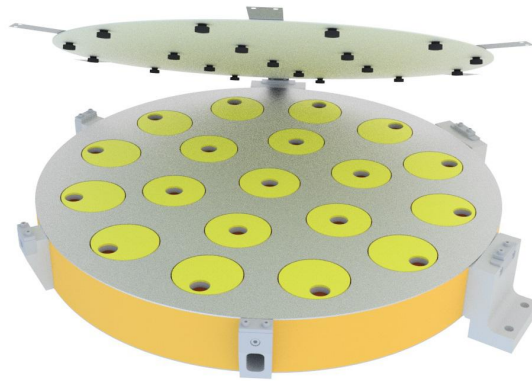
Figure 3. Measurement of the surface roughness

- the structural support for the actuators,

- the reference surface for the deformable mirror (through the capacitive sensors armatures)

- the restraint system for the shell at launch by the Electrostatic Locking system.

The backplane is made by a 50 mm thick CFRP / Aluminum honeycomb, with a spherical shape. A pattern of 55 mm diameter holes are cored into the backplane to insert and mount the actuators assemblies. The actuator is made of a CFRP cylindrical structure that mounts the coil assembly. The top surface of the actuator surrounding the coil is made by an aluminum honeycomb too, topped by a glass disk. The latter is coated to make one of the armature of the capacitor that provides the measurement of the distance with the thin shell back surface. The front surfaces of the actuators are just below the rest of the backplane front surface, which is coated as well to make another armature of a second capacitor system that is used during launch to lock the shell against the backplane by electrostatic force. An insulating layer is deposited on top of the backplane armature to this purpose. Front surface shape accuracy is the manufacturing aspect of the backplane that is critical to the electrostatic locking functionality: we achieved front face shape of 34 μm ptv, 5 μm RMS best fit removed. This accuracy together with the thin shell compliance to low order modes proved to be sufficient to achieve the locking force to safely withstand launch loads. The adopted manufacturing process can be extended to 1m size petal structure. Space qualified materials have been used. Finally, aluminum inserts are embedded on the outer edge of the backplane to provide interfaces to the mirror shells by flexures and to the external support.

3.1.3 The control electronics

The control electronics commands the shape of the TS by using voice coil actuators and capacitive position sensors. The actuators produce a magnetic field that is proportional to the current flowing through a coil. This magnetic field acts on permanent magnets that are glued on the backside of the shell. The backside is metal coated to form one electrode of the capacitive sensors. A metal-coated armature around each actuator represents the second electrode and is used to measure the distance between shell and actuator. A second usage of the coating of the backside of the shell is for an electrostatic locking mechanism. The counter-electrode for the electrostatic locking is the front side of the reference body that is as well metal coated. By applying a large voltage to these two large electrodes, an electrostatic force is produced that pulls the shell towards the reference body. In this way the shell is fixed to the reference body during the launch phase to protect it from the large vibrations and can be released in space by simply switching the high voltage supply off.

With the distance measurement of each actuator and its force exertion on the shell, a control loop is realized, here called local control loop that keeps the shell at the desired distance at each actuator. See block diagram in Figure 5.

Figure 4. Mechanical drawing of the reference body and thin shell, with the 19 magnets and the relative capacitive sensor armatures on the RB.
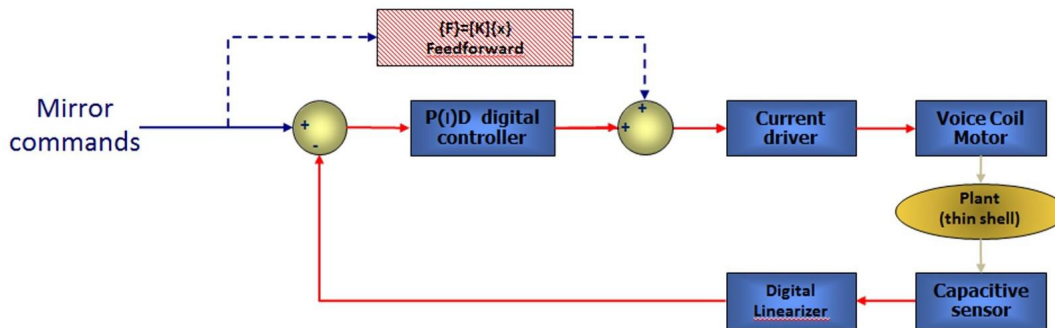

Figure 5. Local control loop.

The mirror command in Figure 5 represents the new position the shell should take at each actuator calculated from a central computational unit. This value is compared to the measured distance value and the difference is fed to a PID regulator. The regulator calculates the required current that has to flow through the coil in order to push or pull the shell in place. This local control loop is implemented in a power efficient 16-bit microcontroller that is on the co-located actuator electronics sitting directly at the actuator and is running with a frequency of about **1.8 kHz**.

The firmware of the microcontroller contains also the possibility to receive as well a force value from the central computational unit to implement the feedforward force functionality in order to speed up the positioning of the shell to a new distance. The central computational unit that calculates the new position commands calculates as well the force required by each actuator to reach the new gap. This speed-up can be used for improving the control performances of the shell in vacuum where no air dumping effect is present and therefore the gain of the local control shall be lowered to guaranty stability.

The power consumption for a space-based telescope is a key parameter and therefore in the LATT project a major attention was given to optimize the actuator electronics for power consumption. The microcontroller program is highly optimized for low power consumption as described in 3.1.4 and we were able to achieve values around **52 mW/actuator** that are better than the initial requirement.

During the test campaign, the LATT prototype was controlled using Matlab running on a PC, which was attached to a Microgate interface board. The interface board uses a multi-drop LVDS bus to interface to the actuator electronics boards.

3.1.4 The actuators

The LATT actuators are called smart actuators because each actuator has its own co-located intelligent electronics to perform the local control loop. Each actuator is composed by a cup as shown in Figure 6 containing the coil, the capacitive sensor armature surrounding the coil and the smart actuator board that houses the electronics.
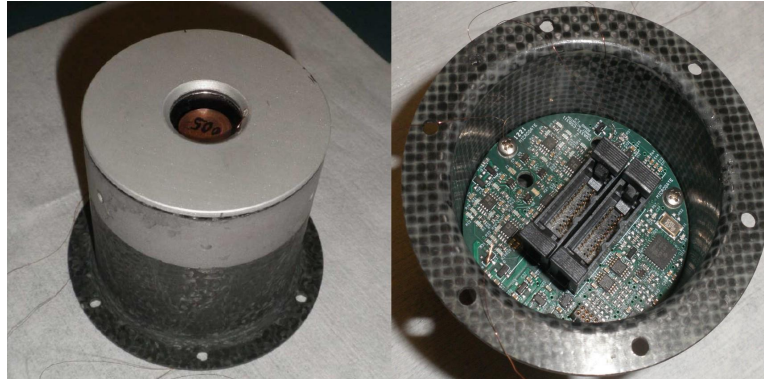

Figure 6. Smart actuator board

Each actuator cup can be easily mounted and dismounted from the reference body. The board is connected with thin wires to the coil and the armature on one side and contains two flat cable connectors to connect to the multi-drop LVDS bus on the other side.

The capacitive sensor signal is amplified and fed to a 16-bit ADC to digitize the capacitance between actuator and TS, which is inversely proportional to the gap. A 16-bit DAC is used to define the setpoint of an analog current loop. Such current source drives the coil that generates a magnetic field, creating a roughly proportional force on the magnets glued on the TS back surface. The current source comprehends four Howland charge pump stages to enable ground-based tests where the gravity acts on the shell; in space where no gravity is present, one driver is enough to control the mirror. The microcontroller reads the ADC value from the capacitive sensor electronics, perforce the calculations for the PID regulation and sends the resulting current value to the DAC. Between these control tasks, the microcontroller handles also the data communication to the interface board to receive the mirror commands and to send back the actual actuators gaps and forces and other telemetry data. To reduce power dissipation the different tasks of the microcontroller are running on different clock frequencies. With these measures a low power consumption of the actuator electronics between 50 mW and 58 mW could be achieved.

The total weight of around **80 g** for each actuator is another remarkable achievement and can be reduced by further optimization.

In order to perform the vacuum tests all components of the smart actuator board including the harness were selected to have low outgassing rates. They are as well suited to withstand the vibration tests and thermal tests as reported in 3.2.

Nevertheless, it shall be remarked that the actuator electronics for the LATT prototype is built with standard off-the-shelf components that are not space qualified in particular concerning the radiation aspects.

3.2 Laboratory test campaign

The OBB has been submitted to the following test sequence to validate and assess the feasibility of the OBB design and the applied technology for future large aperture space telescope. In the following we will give a resum of the test operations and of the results achieved.

3.2.1 Thermal-vacuum test

Thermal testing in air (spanning the 0° C to 40° C temperature range) showed no significant change in the performance of the capSens reading. The only problem related to temperature changes that could be observed

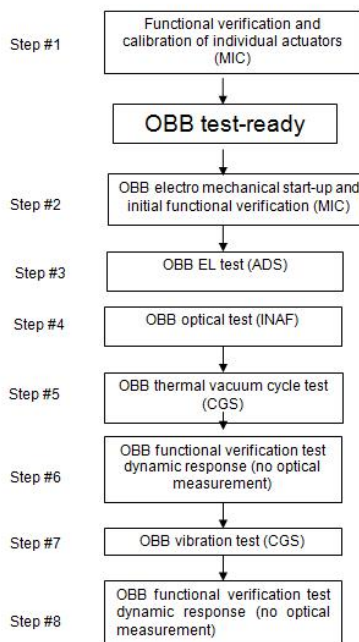| Step #1 | Functional verification and calibration of individual actuators (MIC) |
Step #2	OBB electro mechanical start-up and initial functional verification (MIC)
Step #3	OBB EL test (ADS)
Step #4	OBB optical test (INAF)
Step #5	OBB thermal vacuum cycle test (CGS)
Step #6	OBB functional verification test dynamic response (no optical measurement)
Step #7	OBB vibration test (CGS)
Step #8	OBB functional verification test dynamic response (no optical measurement)

Figure 7. Sequence of the laboratory test campaign.

is the large distance change between shell and reference body related to the high axial stiffness of the flexures and the deformation of the reference body.

The feedforward (FFWD) matrix was acquired to determine the stiffness and the mechanical modes of the shell. The results taken at different temperatures have been compared with the results from the electro-mechanical tests executed at different facilities in previous steps; the main outcome of the feedforward matrix results is that the stiffness matrices do not change significantly with the temperature. After relaxing manually the forces on the flexures (as the flexures over-constrain the shell against the reference body and cause its deformation upon temperature changes), it was necessary to untighten/tighten the flexures at each temperature step to relax the force that the flexures execute on the shell in order to bring the shell again in a good position to the reference body to perform the measurements), the stiffness decreases with decreasing shell distance, which leads to the assumption that the changes in stiffness are related to changes of the shell distance caused by the temperature behavior of the reference body and the flexures. The modal step response tests were executed first on the shell in neutral position hold by the 6 flexures and then for a tilted shell in horizontal and vertical direction. For the environmental tests, the relevant parameter of the modal step response tests is the settling time, which gives information about the dynamic performance of the shell control. Thru the different modal step results, the settling times do not vary significantly with changes of the temperature. Especially when the forces are relaxed and the shell is not too far or too close, the modal step responses can be executed with a large margin of the force required independent on tip-tilt or without. All modal step results at each temperature step show that up to mode 14 the specifications of a settling time <0.72 s within 99% are achieved.

Further the power consumption of the actuators and their control electronics, i.e. the power consumption of the Smart Actuator Boards (SAB), was measured. The consumption has been measured controlling the mirror in closed loop while commanding the positions corresponding to its natural uncontrolled shape. The measured power consumption does not vary significantly at different temperatures independently of the number of used drivers.

All the results show that the LATT is performing well over the entire temperature range of 0° C 40° C when relaxing the forces on the flexures is allowed.
The second part of the thermal testing was the test under vacuum conditions at ambient temperature. The

Figure 8. The thermo-vacuum chamber.

vacuum test has been performed in TVAC chamber of CGS in Milan after the vibration test was performed. The OBB has been installed in vertical configuration (this was the only configuration tested in vacuum) within the chamber, shell vertical pointing the horizon.

All the tests performed in vacuum show that:

- The obtained results (following the vibration tests) showed no degradation of the performance and functionality of the LATT system compared to the tests executed before the vibration tests and with the OBB in climatic chamber. The performance of actuator indirectly accounts for the mechanical performance of the mirror. This means that the electrostatic locking mechanism and other measures that have been designed to protect the shell, electronics and reference body during the demanding vibration tests worked well and no damaged could be observed.

- The tests in vacuum showed that also in vacuum the electronics works fine (CapSens and voice coils worked well) without significant performance drops. The only and already expected problem in vacuum that was observed is the lack of the air damping in the control of the shell. However, this problem was solved by lowering drastically the gain of the PID local control loop setting new parameters in the microcontrollers of the actuators. With this new local control loop parameters again a stable control of the shell was obtained even in vacuum and allowed us to perform successfully all electromechanical tests.

- Because of the lower gain of the local control loop, the modal step settling times increased significantly. The local control loops are stable but much slower. The problem with the vacuum is that the air between shell and reference body is missing. That air dumps down the movements of the shell and acts as stabilizing effect on the control loop (to compensate for the damping effects) slowed down significantly the control. Nevertheless, we believe that our proposed feed-forward force method that is used in ground based telescopes for other reasons can speed-up the control loop under vacuum, in order to replicate the test results obtained in ambient.

- The measured power consumption in vacuum is very close to the measured values in air that already have outperformed our expectations. This is a very positive result considering that the power dissipation limit is one of the most challenging aspect of the project especially considering the space application

- At the door opening no deposition on the mirror was formed. This confirms that the white deposition found on the mirror after TVAC test in SERMS (Terni) could be caused from the degassing of parts inside the SERMS vacuum chamber itself.

3.2.2 Vibration test

The OBB successfully underwent a vibration test campaign in line with space standard to demonstrate the capability of the OBB to withstand the vibration environment without structural yielding or failure and without degradation of performances. Further the capability of the Electro static locking to keep safely the mirror under

Frequency	Level
Sine level	
5 -15 Hz	
15-50 Hz	10 g
50-80 Hz	6 g
800-100 Hz	3.5 g
Random Spectrum	
20 -110 Hz	+3dB/octave
110-700 Hz	0.09 [g²/Hz]
700 2000 Hz	-3 dB/octave

Table 3. Qualification spectra.

Excitation axis	MP2 acceleration limit along the axis		
	Full level random test [g RMS]	Mid level random test [g RMS]	Low level random test [g RMS]
X	$7.22 < a < 7.99$	$3.61 < a < 3.99$	$1.80 < a < 1.99$
Y	$6.33 < a < 7.0$	$3.16 < a < 3.5$	$1.58 < a < 1.75$
Z	$9.93 < a < 10.98$	$4.96 < a < 5.49$	$2.48 < a < 2.74$

Table 4. Acceleration limits.

the vibration environment that the OBB will experience during the launch phase has been successfully verified. Two configurations have been considered to vibrate the OBB in the three directions: Shaker coupled with slip table to vibrate the in plane axes (X and Y) and shaker only to vibrate the out of plane axis (Z). The unit has been tested with external harness and powered off for all the test duration with the EL powered on.
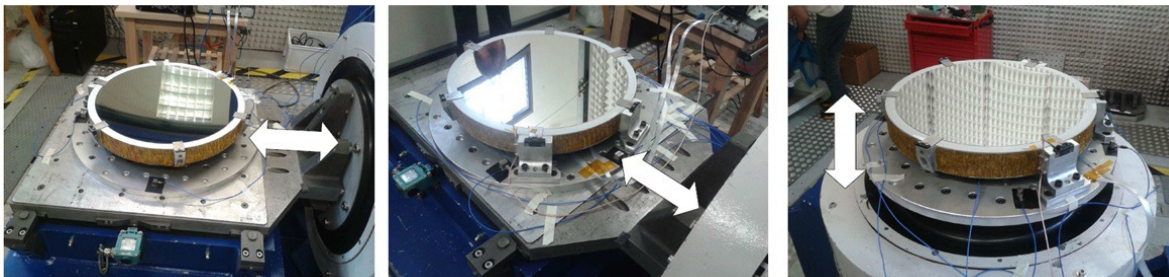

Figure 9. The vibration testbed, indicating the directions of the excitations applied.

The test adapter is designed to guarantee that the input vibration levels are transmitted from the exciter to the OBB without relevant amplification/degradation. The fixture is composed by a round plate and three pads are fixed on top of it by means of 3 countersunk screws.
The OBB has been subjected to the following sine qualification levels separately along the three orthogonal axes and also to the following random notched qualification spectrum level, with a test duration on each axis of 2.5 minutes. The notching has been implemented to not exceed the OBB CoG acceleration of 13.9 g 5% (3 sigma value) that is the acceleration that the petals composing the primary mirror of the telescope on board of the satellite will experience when the satellite will be subjected to the acoustic qualification load incremented by a 1.2 factor.

The reading of the accelerometers has been monitored and limited to the acceleration of the CoG accoding to the indications in Tab.4. indications :

The qualification vibration test has been concluded successfully and the pass/fail criteria satisfied.

The Electrostatic locking was able to keep safely the shell during the vibration along the three axes demon-

strating the robustness of the design. Some scratches on the back surface of the shell and on the front face of the backplane have been detected at the end of the test during the de-integration of the shell. The functionality of the EL was not affected by these signs.

The tests have demonstrated the adequacy of the selected technologies for the future development of the large aperture space telescopes

3.2.3 Optical qualification

The goal of the optical test was to demonstrate the controllability of the thin shell surface with the very low actuator density and power budget of the OBB. The mirror was installed on the bench with optical axis horizontal and measured at its center of curvature. The interferometer was a dynamic 4D-Technology Twyman-Green. The first step after optical alignment was the regulation of the lateral blades in order to minimize their impact on the surface shape. Then we collected the phase maps corresponding to the mirror stiffness modes and we piled them up to build the optical interaction matrix M of the OBB on the bench. The phase maps in M are shown in Fig.10. The matrix M was used to run the flattening procedure, which consists in the minimization of the Wavefront error (WFE) within the visible area by applying the mirror modes in M. The actuator command to flatten the current WFE w is computed as $c_{flat} = -M^+ w$, where M^+ is the pseudo-inverse of M.

Within this scope, we were not interested in the final WFE achieved in the laboratory. Such result is, in facts, not representative of the optical quality of a LATT primary mirror in 0-g environment. For instance, the thin shell was hold by flexures to avoid any lateral displacement during laboratory testing and the deformation induced by such over-constraint on the optical surface was beyond the actuator correction space. To this purpose, we tested the flattening on a smaller area where the effect of the flexures was lower. Such procedure allowed us to investigate the optical controllability and the WF correction in a more representative context. We considered two test cases: in the first, we flattened the shell over an area with 296 mm diameter, achieving a final WFE of $\approx$ 90 nm RMS. In the second, more interesting setup, we considered the patch controlled by 7 actuators (located on a hexagon and at its center) over an area of 180 mm diameter: the flattening converged to 26 nm RMS. We compared such result with a typical flattening realization ($\approx$ 20 nm RMS) on the Large Binocular Telescope adaptive secondary; we considered a patch with the same actuator geometry but with a diameter of 60 mm (instead of 180 as for the OBB). The test demonstrated that it is possible to control the WFE of a thin glass shell with a low actuator density and low power budget. A more detailed discussion on the optical test may be found in[3] and more on the optical calibration procedure applied to adaptive mirrors in[4] and in.[5]
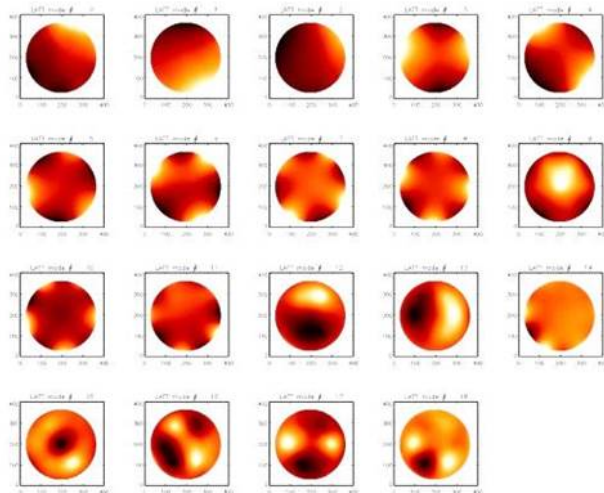

Figure 10. Phase maps of the mirror stiffness modes as measured with the interfeometer.

LATT OBB

LBT TS#4

Diam: 20 cm
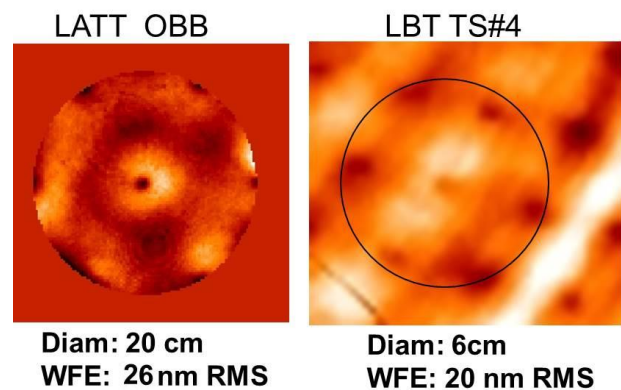WFE: 26 nm RMS

Diam: 6cm
WFE: 20 nm RMS

Figure 11. Comparison between the flattening with 7 actuators on the OBB and at the LBT.

4. LATT AND OBB ASSESSMENT: CRITICAL ANALYSIS AND PERSPECTIVES

At the end of the LATT project, we can claim the main objectives of the study and prototyping have been pursued and that the concept is a fitting approach for space active optics. We will try now to outline the study and prototyping results in order to assess the technology.

4.1 Concept assessment from initial study

The concept of deformable mirror, composed by a TS shaped by voice coil actuators has been demonstrated in the last years on 1m class adaptive secondaries, like the LBT (where two TS are currently in operation and offered for scientific observations) and VLT (the DSM replacing the Dornier rigid secondary is currently in commissioning at ESO-Garching). From this perspective we can conclude with the following remarks.

- The working principle has been fully assessed in terms of safety, reliability and image quality at typical observing conditions for ground based observatory.

- The manufacturing of medium to large size TS (diameter 0.5 m to 1 m, thickness 1 mm to 2 mm) is mature and able to deliver a remarkable optical quality apart from the very low order modes after the thinning process.

- The active flattening with contactless actuators is able to deliver a final WFE within 15 to 30 nm RMS typical: contemporary flattening and active phasing of a segmented deformable mirror has been also demonstrated and will be extensively performed on the E-ELT adaptive M4 mirror.

- Voice coil actuators are intrinsically fail-safe as they are contactless: in case of an unrecoverable failure, they may be disable without introducing a *hard point* on the optical surface.

- The choice of putting the WF corrector at the primary presents a number of benefits, for instance the simplification of the optical design and the delivery of a corrected WF to the entire optical train.

- The deformable mirror equipped with TS and contactless actuators is naturally suitable for low mass implementations, thanks to the fact that the mechanical support is physically detached from the Zerodur optical surface, this allowing the use of ultra-lightweight materials.

- The possibility to polish the TS according to any optical prescription makes the LATT a flexible tool to fit a specific science requirement and mission scenario.

4.2 OBB results

The OBB worked well as a technical demonstrator of the space active primary concept with the LATT. In particular the following points were successfully assessed.

- The electrostatic adhesion mechanism is able to lock the TS onto the RB and prevent it from detaching and crashing during the launch phase.

- The TS may be actively controlled and flattened with a very limited actuators power budget and an internal metrology with low bandwidth.

- The TS may be stably controlled in vacuum, i.e. with no air damping (as it was necessary for fast adaptive mirrors).

- The TS may be stably controlled and flattened with a low actuator density, the final WFE being comparable when flattening with 7 actuators a 6x6cm (LBT case) and 20x20 cm area (OBB).

- A lightweight system (with areal density as low as 17 kg/m2) may be assembled without prejudice to the optical quality.

- The system has been successfully tested in a range of relevant temperature conditions.

4.3 Upgrades path

As already mentioned, the OBB was intended as a technical demonstrator. For this reason, a number of items were optimized within the scope of the verification tests only, not as to equip a final unit. We are now ready to divert our attention to such aspects and propose a suitable upgrade.

- The actuator electronics shall be space qualified either by changing the components to space qualified ones where applicable or by qualifying some devices for space.

- The lateral flexures are required for 1-g testing but their need is less important once in orbit. Both the flexures and their mounts shall be carefully designed as to not provide an over-constraint on the glass. In particular, while the gluing had a negligible impact of the image quality, the flexures could not be regulated in position, so that the optical verification was done far from the zero-stress condition. An updated flexures design could involves a dynamic (set and forget) deployment mechanism or even an unlocking device to completely release the shell when the actuator loop is closed.

- The possibility of a central flexures shall be taken in mind, especially as a primary mirror has a central hole to let the beam in. The impact of such central membrane could be moderate when the affected area is within the M2 obstruction.

- Although the areal density is low, a further mass reduction could be feasible. This goal may be achieved either with a conservative strategy (i.e. re-design/machine some items which could be easily lightened) or with a more radical approach, including a new system architecture. We estimate that an areal density in the range 10 to 15 kg/m2 could be reached.

- In the current implementation, the system was tested with the optical axis horizontal, in order to minimize the gravity induced self-bending, which cannot be compensated with the OBB actuators areal density. The system could in principle be tested also with vertical optical axis, by means of charging the TS and the RB with the same polarity to compensate for the TS weight.

- A study concerning the best actuators geometry with a given TS shape could yield a valuable knowledge for assessing the case of hexagonal (e.g.) petals of a segmented aperture.

- We could identify a strategy to obtain a decent WF even with disabled actuators. This could include a more demanding approach to the TS polishing, a complete revision of the flexures and a larger distance between the RB and the TS.

- A WF sensing strategy should be studied, matching the peculiar features of the LATT primary. We take inspiration from the FLAO system at the LBT, where the adaptive secondary is coupled with a pyramid WFS to deliver diffraction limited images of the 8.4 m telescope.

4.4 Future development

We could envision two development paths for the LATT as an active space primary. As a first strategy, the OBB could be expanded to become a 1 m class active mirror. At a first order, it has been demonstrated with the LBT adaptive secondary prototype, it is just matter of producing a larger TS and populating a larger RB with actuators.

As a second strategy, we could start thinking a segmented aperture, where a large size deployable mirror fits the launcher fairing thanks to smaller sized, folded together petals. In this scenario, the large actuator stroke, together with a suitable phasing algorithm, may take care of the segments alignment, thus de-rating the requirements on the deployment system.

5. CONCLUSION

Within the LATT project we investigated a strategy for the active wavefront correction of a space telescope. We proposed to extend the development and operational expertise matured in the field of ground based adaptive optics; in particular, we tailored the concept of the adaptive secondary mirror to match the requirements of a space active primary. The system is composed by a thin Zerodur shell, which is shaped by contactless voice coil actuators controlled in close loop by capacitive sensors. Such approach offers many advantages, namely: the surface shaping at the entrance pupil, to deliver a corrected WF to the rest of the optical train; a concept which may be adapted to fit the telescope design and is suitable for segmentation; a fail-safe optical control via contactless, voice coil actuators able to provide a 1 mm stroke, which is helpful for the in orbit phasing of a segmented aperture.

A demonstration prototype mirror of 40 cm diameter, controlled by 19 actuators with a final areal density of 17 kg/m2, has been manufactured and tested to assess the concept and push the TRL toward 5. In particular, we demonstrated its optical controllability with low actuator density and power budget; on the vibration bench, we validated the electro-static locking mechanism to guarantee the thin shell safety exposed to the launch accelerations.

The project was a response to an ESA call under TRP programme.

REFERENCES

[1] Mazzinghi, P., Bratina, V., Ferruzzi, D., Gambicorti, L., Simonetti, F., Zuccaro Marchi, A., Salinari, P., Lisi, F., Olivier, M., Bursi, A., Gallieni, D., Biasi, R., and Pereira, J., "Deployable, lightweight, and large aperture spaceborne telescope for lidar-based earth observations," in [*Lidar Technologies, Techniques, and Measurements for Atmospheric Remote Sensing III*], *Proc. of SPIE* **6750**, 67500X (Oct. 2007).

[2] Riccardi, A., Xompero, M., Briguglio, R., Quirós-Pacheco, F., Busoni, L., Fini, L., Puglisi, A., Esposito, S., Arcidiacono, C., Pinna, E., Ranfagni, P., Salinari, P., Brusa, G., Demers, R., Biasi, R., and Gallieni, D., "The adaptive secondary mirror for the Large Binocular Telescope: optical acceptance test and preliminary on-sky commissioning results," in [*Adaptive Optics Systems II*], *Proc. of SPIE* **7736**, 77362C (July 2010).

[3] Briguglio, R., Xompero, M., and Riccardi, A. & al.., "Development of large aperture telescope technology (LATT): test results on a demonstrator bread-board," in [*International Conference on Space Optics*], (2014).

[4] Briguglio, R., Xompero, M., and A.Riccardi, [*Optical calibration of adaptive mirrors*], Osservatorio Astrofisico Arcetri, Firenze (2016).

[5] Briguglio, R., Xompero, M., and Riccardi, A. & al.., "Optical calibration and test of the VLT Deformable Secondary Mirror," in [*Proceedings of the Third AO4ELT Conference*], Esposito, S. and Fini, L., eds., 105 (Dec. 2013).